Altered Expression of *Raet1e*, a Major Histocompatibility Complex Class 1–Like Molecule, Underlies the Atherosclerosis Modifier Locus *Ath11* 10b

José M. Rodríguez, **Susanne Wolfrum**, **Megan Robblee**, **Kwan Y. Chen**, **Zachary N. Gilbert**, **Jae-Hoon Choi**, **Daniel Teupser**, and **Jan L. Breslow**

Laboratory of Biochemical Genetics and Metabolism (J.M.R., S.W., M.R., K.Y.C., Z.N.G., D.T., J.L.B.) and Laboratory of Cellular Physiology and Immunology (J.-H.C.), Rockefeller University, New York, NY; Department of Life Science, College of Natural Sciences, Hanyang University, Seoul, Republic of Korea (J.-H.C.); and Institute of Laboratory Medicine, University Hospital Munich, Ludwig-Maximilians-University, Munich, Germany D.T.)

Abstract

Rationale—Quantitative trait locus mapping of an intercross between C57.*Apoe*$^{-/-}$ and FVB.*Apoe*$^{-/-}$ mice revealed an atherosclerosis locus controlling aortic root lesion area on proximal chromosome 10, *Ath11*. In a previous work, subcongenic analysis showed *Ath11* to be complex with proximal (10a) and distal (10b) regions.

Objective—To identify the causative genetic variation underlying the atherosclerosis modifier locus *Ath11* 10b.

Methods and Results—We now report subcongenic J, which narrows the 10b region to 5 genes, *Myb*, *Hbs1L*, *Aldh8a1*, *Sgk1*, and *Raet1e*. Sequence analysis of these genes revealed no amino acid coding differences between the parental strains. However, comparing aortic expression of these genes between F1.*Apoe*$^{-/-}$ Chr10SubJ$^{(B/F)}$ and F1.*Apoe*$^{-/-}$ Chr10SubJ$^{(F/F)}$ uncovered a consistent difference only for *Raet1e*, with decreased, virtually background, expression associated with increased atherosclerosis in the latter. The key role of *Raet1e* was confirmed by showing that transgene-induced aortic overexpression of *Raet1e* in F1.*Apoe*$^{-/-}$ Chr10SubJ$^{(F/F)}$ mice decreased atherosclerosis. Promoter reporter constructs comparing C57 and FVB sequences identified an FVB mutation in the core of the major aortic transcription start site abrogating activity.

Conclusions—This nonbiased approach has revealed *Raet1e*, a major histocompatibility complex class 1–like molecule expressed in lesional aortic endothelial cells and macrophage-rich regions, as a novel atherosclerosis gene and represents one of the few successes of the quantitative trait locus strategy in complex diseases.

Keywords

atherosclerosis; gene expression; genetic susceptibility; mice; mouse model; quantitative trait loci

Atherosclerotic cardiovascular disease is the major cause of death and disability in Westernized countries and is fast becoming a public health problem in the developing world.[1] Atherosclerotic cardiovascular disease is considered a complex genetic disease with many genes involved and with important environmental influences and gene–environment interactions.[2] In humans, the advent of high-density single nucleotide polymorphism (SNP) chips made possible genome-wide association studies of atherosclerotic cardiovascular disease risk factors, such as high low-density lipoprotein (LDL), low high-density lipoprotein (HDL), high triglycerides, hypertension, diabetes mellitus, and obesity, as well as genome-wide association studies of coronary heart disease and myocardial infarction.[3] These studies in humans can be complemented by genetic studies in animal models, in which genes directly influencing the atherosclerosis phenotype itself can be identified.[4] Mouse models of atherosclerosis, such as $Apoe^{-/-}$ and $Lldlr^{-/-}$ mice, have been successfully used to assess the influence of candidate genes on the progression and regression of atherosclerotic lesions.[5] Attempts have also been made to use reverse genetic approaches to discover new genes and pathways involved in atherosclerosis and other complex traits. Intercrosses and backcrosses between strains varying in complex disease-related traits have been performed, and quantitative trait locus (QTL) mapping has been used to identify modifier loci.[6] This approach has resulted in mapping by linkage analysis of ≈4000 mouse QTLs, including the identification of 44 atherosclerosis modifier loci, generally called *Ath* loci.[7] Identifying the causative gene of a QTL requires confirmation of the locus in congenic mice and subsequent narrowing of the region in subcongenic mice. Finally, only by identifying the causative variation and showing how it acts to alter gene function in a manner that changes the phenotype can one be certain of the culprit gene.[8] However, despite this wealth of genetic information, QTL studies have rarely progressed beyond the initial QTL analysis, and only a few of these QTLs have been identified at the molecular level as specific genes or noncoding elements.[9]

We have used the $Apoe^{-/-}$ mouse model in a QTL analysis crossing the atherosusceptible strain C57BL/6 (abbreviated C57 or B) with the atheroresistant strain FVB/N (abbreviated FVB or F) to identify the *Ath11* locus in the proximal region of mouse chromosome 10.[10–13] This strong atherosclerosis locus, corresponding to the proximal 21 cM of chromosome 10, in which the FVB allele acts as an atherosusceptible recessive allele, was verified in congenic mice. To confirm this interval as an atherosclerosis-modifying locus, we apply a novel strategy of using F1 mice to allow interactions between C57 and FVB alleles across the genome that may be crucial for the development of the atherosclerosis phenotype.[14] Subsequent creation and characterization of 11 subcongenic lines revealed *Ath11* to be complex, with a 10a proximal region (between 0 and 7.3 Mb) in females containing 21 genes, including the strong candidate *Esr1*, and a 10b distal region (between 20.3 and 22.1 Mb) in both sexes containing only 7 genes (*Pde7b, Ahi1, Myb, Hbs1L, Aldh8a1, Sgk1*, and *Raet1e*).[15]

We now report further narrowing of the *Ath11* 10b region to only 5 genes (*Myb, Hbs1L, Aldh8a1, Sgk1*, and *Raet1e*) by isolation and characterization of an additional subcongenic line. Furthermore, extensive sequence and expression analysis uncovered altered *Raet1e* gene expression underlying the *Ath11* 10b locus, which was confirmed by creation of *Raet1e* transgenic mice. Finally, the molecular basis for altered aortic *Raet1e* expression and its atherosclerosis phenotype was revealed to be a mutation in the transcription initiation region of the *Raet1e* gene. Our nonbiased approach has identified *Raet1e*, a major histocompatibility complex class 1–related molecule, as a novel atherosclerosis modifier gene and represents one of the few successes of the QTL strategy in complex disease.

Methods

A detailed description of Materials and Methods is provided in the Online Data Supplement.

Mice

$Apoe^{-/-}$ and $Ldlr^{-/-}$ mice on different backgrounds were derived at Rockefeller University. Mice were named as follows: strain; atherosclerosis-sensitizing background; subcongenic line; and genotype of the Chr10 interval, for example, F1.$Apoe^{-/-}$Chr10SubI$^{(B/F)}$ for heterozygous F1 (C57/FVB) (B/F) mice on the $Apoe^{-/-}$ background that were heterozygous (B/F) for the subcongenic I (SubI) region.

Generation of a Narrowed Subcongenic Interval Mouse Line for Atherosclerosis Studies

To narrow the $Ath11$ 10b locus region, subcongenic strains containing a reduced portion of the original interval were generated by crossing B6.$Apoe^{-/-}$ Chr10SubI$^{(B/F)}$ with B6.$Apoe^{-/-}$. A recombinant missing part of the original FVB interval was identified by genotyping the genetic markers D10mit213 and D10mit16 that delimit SubI.[15] The mouse line with the shortened interval was named subcongenic J (SubJ; B6.$Apoe^{-/-}$ Chr10SubJ$^{(B/F)}$). This new line was bred with FVB.$Apoe^{-/-}$ mice to generate littermates that were either F1.$Apoe^{-/-}$ Chr10SubJ$^{(F/F)}$ or F1.$Apoe^{-/-}$ Chr10SubJ$^{(B/F)}$ for atherosclerosis studies.

Generation of BAC-*Raet1e* Transgenic Mice

A 56 016-bp Not I fragment containing only the C57-*Raet1e* gene was isolated, purified, and introduced by pronuclear microinjection into FVB-fertilized eggs. Three founder mice, FVB.Tg*Raet1e*22, FVB.Tg*Raet1e*26, and FVB.Tg*Raet1e*30, were backcrossed 2 generations to FVB.$Apoe^{-/-}$ mice to obtain FVB.$Apoe^{-/-}$ Tg*Raet1e* mice. All 3 FVB.$Apoe^{-/-}$ Tg*Raet1e* transgenics were bred to B6.$Apoe^{-/-}$ Chr10SubJ$^{(B/F)}$ mice to generate the F1 (B6/FVB) littermates suitable for atherosclerosis studies.

Mouse Feeding, Atherosclerosis Assessment, and Blood Analysis

For atherosclerosis studies and gene expression analysis, mice were weaned at 28 days of age and fed a semi-synthetic modified AIN76a diet containing 0.02% cholesterol. Animals were fasted for 6 hours and euthanized at 6 and 16 weeks of age for the gene expression analysis and at 16 weeks of age for all atherosclerosis lesion studies as described.[11, 15]

RNA Isolation, cDNA Synthesis, and Quantitative Fluorogenic Reverse Transcription Polymerase Chain Reaction

Total RNA was extracted from whole aortas (ascending aorta through abdominal aorta after removing the adventitia) and livers of mice using TRIzol reagent (Invitrogen). RNA was reverse-transcribed into cDNA using SuperScript III Reverse Transcriptase (Invitrogen) and random hexamer primers.

Quantitative fluorogenic reverse-transcription polymerase chain reaction was performed in an ABI PRISM 7900 Sequence Detection System (Applied Biosystems). Specific primers and probes for every gene were selected to span 2 exons to avoid coamplification of genomic DNA. mRNA expression levels were normalized to the housekeeping gene *cyclophilin A*.

Aortic *Raet1e* Rapid Amplification of 5′ End of cDNA Polymerase Chain Reaction

The rapid amplification of 5′ end of cDNA System for Rapid Amplification of cDNA Ends (Invitrogen) was used for 5′ cDNA end amplification of *Raet1e* according to the manufacturer's instructions.

Assessment of *Raet1e* Promoter Functionality by Dual-Luciferase Reporter Assay

The *Raet1e* promoter fragments of FVB and C57 genomic DNA upstream of the major aortic transcription start site (TSS)-1 were cloned into the luciferase reporter vector pGl4.11[luc2CP] (Promega). Site-directed mutagenesis was used to introduce separately, into the C57 promoter D fragment, each of the 4 FVB sequence variations present in the first 426 bp of promoter and the C57 variant of SNP rs50817078 (JMRv10073) into the FVB promoter D fragment. C57SV002 (Jackson Laboratory), BalbcSV006 (Jackson Laboratory), and NIH3T3 (ATCC) cells were cotransfected with the expression vectors and the vector pGl4.74[hRluc/TK] (Promega). Luciferase activities were measured using the Dual-Luciferase Reporter Assay System (Promega).

Results

Narrowing the *Ath11* 10b Region: SubJ

The distal 10b region of the original *Ath11* locus, containing a proatherogenic FVB allele, was defined by obtaining and characterizing SubI,[15] which contained 7 genes (Figure 1A). We now report a new recombinant SubJ, which was derived from SubI (Figure 1A and Online Figure I). Fine-mapping revealed that SubJ is delimited at its proximal end by the SNP rs29318728 at 21 148 321 bp. This SNP is in *Myb* intron 8; so, SubJ contains the *Myb* promoter and potentially some of the first 8 exons of the 15-exon gene (Online Figure Ia). SubJ is delimited at its distal end by SNP rs108701952 at 22 170 993 bp. This SNP is in *Raet1e* intron 2; so, SubJ contains the *Raet1e* promoter and the noncoding exons 1A and 1B (Online Figure IB). Therefore, compared with SubI, SubJ excludes *Pde7b, Ahi1*, and a portion of the *Myb*-coding region and contains the rest of *Myb, Hbs1L, Aldh8a1, Sgk1*, and *Raet1e* promoter.

We next determined whether SubJ contained the *Ath11* 10b atherosclerosis susceptibility region. Aortic root lesion area was assessed in F1 mice that were heterozygous (C57/FVB) in the SubJ region (F1.$Apoe^{-/-}$ Chr10SubJ$^{(B/F)}$) and in F1 mice carrying homozygous FVB alleles in the SubJ region (F1.$Apoe^{-/-}$ Chr10SubJ$^{(F/F)}$). In both sexes, F1.$Apoe^{-/-}$ Chr10SubJ$^{(F/F)}$ mice had significantly larger lesions than F1.$Apoe^{-/-}$ Chr10SubJ$^{(B/F)}$ mice (males: 76%, $P<0.0001$; females: 60%; $P<0.004$; Figure 1B). This is similar to what we previously reported for SubI and confirms that SubJ contains the *Ath11* 10b atherosclerosis susceptibility region carrying a proatherogenic FVB allele. F1.$Apoe^{-/-}$ Chr10SubJ$^{(B/F)}$ and F1.$Apoe^{-/-}$ Chr10SubJ$^{(F/F)}$ mice did not differ in total and HDL cholesterol levels (Online Table I).

Attempts to Further Narrow the SubJ Region

Mouse genetic maps until 2009 indicated that SubI, delimited by D10mit213 and D10mit16, spanned 3.2 cM. Thus, attempts were made to identify recombinants to narrow this region. We obtained SubJ as discussed, but further attempts examining 541 meioses derived by breeding subcongenics E, I, and J failed to identify any new recombinants. A more recent genetic map[16] indicates that the distance between D10mit213 and D10mit16 is only 0.07 cM (Online Figure II). Thus, it is remarkable that we were able to derive SubJ, but the short genetic distance explains our failure to derive new recombinants and caused us to abandon this approach to further narrow the interval. We also attempted the yin-yang cross strategy,

using a third mouse strain, to narrow the *Ath11* 10b region. The atherosclerosis susceptibility locus at proximal chromosome 10 was not identified in a cross between C57 and BALB/c strains on the *Ldlr*$^{-/-}$ background.[17] Therefore, we hypothesized that the proatherosclerosis variation in this region in FVB was absent in BALB/c. Sequence comparison indicated that FVB and BALB/c are highly similar in this region (<0.5% of the known SNPs in the mouse database in this region are polymorphic between FVB and BALB/c), so any differences might be candidates for the culprit causative variation. Unfortunately, when we actually crossed BALB/c and SubJ (Online Figure III), we found that BALB/c also carried the proatherogenic allele at this modifier locus (Online Figure IV), which made the few sequence differences between FVB and BALB/c in this region useless for identifying the culprit variation in the *Ath11* 10b region.

Sensitizing Background and the *Ath11* 10b Region

To evaluate the role of the sensitizing background on the atherosclerosis effect of the *Ath11* 10b region, SubJ was intercrossed from the *Apoe*$^{-/-}$ onto the *Ldlr*$^{-/-}$ background, generating F1.*Ldlr*$^{-/-}$ Chr10SubJ$^{(B/F)}$ and F1.*Ldlr*$^{-/-}$ Chr10SubJ$^{(F/F)}$ mice. Aortic root lesion area was assessed in F1.*Ldlr*$^{-/-}$ Chr10SubJ$^{(B/F)}$ and F1.*Ldlr*$^{-/-}$ Chr10SubJ$^{(F/F)}$ mice; in both sexes, F1.*Ldlr*$^{-/-}$ Chr10SubJ$^{(F/F)}$ mice had significantly larger lesions than F1.*Ldlr*$^{-/-}$ Chr10SubJ$^{(B/F)}$ mice (males: 70%, *P*<0.0032; females: 78%; *P*<0.0004; Figure 1C). As shown previously, on the *Apoe*$^{-/-}$ background, F1.*Ldlr*$^{-/-}$ Chr10SubJ$^{(B/F)}$ and F1.*Ldlr*$^{-/-}$ Chr10SubJ$^{(F/F)}$ did not differ in total and HDL cholesterol levels (Online Table I). Thus, the proatherogenic FVB allele present in SubJ, which represents the new shorter *Ath11* 10b region, is independent of the atherosclerosis-sensitizing background, operative in both sexes, and is independent of the total and HDL cholesterol levels.

Sequence Analysis of SubJ Genes and Comparison of C57 and FVB Sequences

To determine the molecular basis of the *Ath11* 10b region, sequence comparison of the 5 SubJ genes between C57 and FVB was undertaken (Table and Online Table II). We initially looked for coding variation. Although there was a coding variation for *Myb* (rs29363766 Q504R), it was in exon 12 outside the SubJ region. There were also 2 sequence variations in the *Sgk1*-coding region, but these did not change the amino acid sequence. In the absence of coding variation within the bounds of SubJ, our attention turned to variations in regions that might affect gene expression. There were sequence variations in the promoter regions of all 5 genes, as well as the 5′ untranslated region (UTR) of the *Hbs1L* and *Raet1e* genes and the 3′-UTR of the *Aldh8a1* gene. Thus, in the absence of coding variation and the presence of numerous potential regulatory variants, it is likely that gene expression differences between C57 and FVB account for the atherosclerosis effect of the *Ath11* 10b region.

Gene Expression Analysis of SubJ Genes

Taqman-specific assays were used to assess the gene expression of the 5 *Ath11* 10b region genes (Online Table III). Aortic expression was compared between F1.*Apoe*$^{-/-}$ Chr10SubJ$^{(B/F)}$ and F1.*Apoe*$^{-/-}$ Chr10SubJ$^{(F/F)}$ in male and female mice at 16 weeks of age (Figure 2). Aortic expression of *Aldh8a1* was undetectable in either strain in both sexes. *Myb, Hbs1L*, and *Sgk1* were expressed in aorta, but no differences between the strains were observed in either sex. In contrast, the *Raet1e* gene showed a large difference in expression, with an order of magnitude less than *Raet1e* expression in both male and female F1.*Apoe*$^{-/-}$ Chr10SubJ$^{(F/F)}$ compared with F1.*Apoe*$^{-/-}$ Chr10SubJ$^{(B/F)}$ mice (Figure 2A and 2B, respectively). Identical results were obtained for aortic expression of the 5 *Ath11* 10b region genes when male and female SubI mice were analyzed comparing F1.*Apoe*$^{-/-}$ Chr10SubI$^{(B/F)}$ and F1.*Apoe*$^{-/-}$ Chr10SubI$^{(F/F)}$ mice at 16 weeks of age (Online Figure VA).

Because 16-week-old F1.$Apoe^{-/-}$ Chr10SubJ$^{(F/F)}$ mice have larger lesions than F1.$Apoe^{-/-}$ Chr10SubJ$^{(B/F)}$ mice, gene expression analysis was also performed in prelesional 6-week-old male and female mice to avoid possible effects on gene expression produced by the disparate atherosclerosis lesion severity observed between strains. Essentially, similar results were found to those of the 16-week-old mice (Figure 2C and 2D), with no significant differences in the expression between the strains, except for the large difference seen in the expression of the *Raet1e* gene.

The liver gene expression profile of the 5 *Ath11* 10b region genes was also compared between F1.$Apoe^{-/-}$ Chr10SubJ$^{(B/F)}$ and F1.$Apoe^{-/-}$ Chr10SubJ$^{(F/F)}$ male and female mice at 16 weeks of age. In contrast to aortic expression, mRNA expression was detected for all 5 genes in the liver of both strains, with a moderate but significant difference in the expression of *Aldh8a1* (1.3-fold; *P*=0.0313) and *Raet1e* (1.6-fold; *P*=0.0037) but not in the other 3 genes (Online Figure VB).

Raet1 comprises a gene family that shares 90% sequence identity among its members. Analysis of the genomic sequence of the *Raet1* exon 6 region showed that C57 mice contained *Raet1g, Raet1d*, and *Raet1e* isoforms, and FVB mice contained *Raet1a, Raet1b*, and *Raet1g* isoforms (Online Figure VIA). As a result of the location of the recombination at the distal end of SubI and SubJ (5′-UTR of *Raet1e*), both F1 strains (F1.$Apoe^{-/-}$ Chr10SubJ$^{(B/F)}$ and F1.$Apoe^{-/-}$ Chr10SubJ$^{(F/F)}$) have the same *Raet1* repertoire, which includes *Raet1a, Raet1b, Raet1g, Raet1d*, and *Raet1e* (Online Figure VIB). The previous gene expression analysis involved the *Raet1e* isoform because, as was described, SubJ contained the promoter and the 5′-UTR region of *Raet1e*. To examine the expression of the other members of this gene family, a probe was used that detects *Raet1a, Raet1b, Raet1g*, and *Raet1d*, but not *Raet1e* (Online Figure VII and Online Table III). As shown in Online Figure VIIIA, the level of expression of *Raet1e* is comparable in magnitude with the level of expression of the other family members combined. Differences in the expression of the other *Raet1* gene family members between aortas of F1.$Apoe^{-/-}$ Chr10SubJ$^{(B/F)}$ and F1.$Apoe^{-/-}$ Chr10SubJ$^{(F/F)}$ mice at 16 and 6 weeks of age were not observed (Online Figure VIIIB).

Raet1e is usually expressed in distressed cells, and we wondered whether the stress of hypercholesterolemia on the $Apoe^{-/-}$ background was required to bring out the difference between genotypes. Therefore, we assessed *Raet1e* expression in mice on the $Apoe^{+/+}$ background, comparing F1.Chr10SubJ$^{(B/F)}$ and F1.Chr10SubJ$^{(F/F)}$ mice. We were able to detect the expression of *Raet1e* in aortas of $Apoe^{+/+}$ mice and found expression at significantly higher levels in F1.Chr10SubJ$^{(B/F)}$ (3.6-fold; *P*=0.0087; Online Figure VIIIC). Therefore, the elevated expression of aortic *Raet1e* in F1.Chr10SubJ$^{(B/F)}$ mice is independent of the stress of hypercholesterolemia, and the latter is not required to bring out the difference between the strains in *Raet1e* expression.

The gene expression analysis strongly suggests that *Raet1e* is the culprit gene behind the atherosclerosis-susceptible locus *Ath11* 10b region, with decreased *Raet1e* expression resulting in increased atherosclerosis lesion area.

Raet1 Protein Is Expressed in Aortic Cells

We investigated Raet1 protein expression in the aortic root of mice. Immunohistochemical analysis (Figure 3A and 3B and Online Figure IXA and IXB) using Raet1 antibodies, which recognize all members of the Raet1 family, revealed that Raet1 protein is expressed in the aorta. Raet1 could be detected in aortic endothelial cells and in the core of atherosclerotic lesions within macrophage-rich regions.

Further analysis of Raet1 expression in aortic cells from F1.*Apoe*$^{-/-}$ Chr10SubJ$^{(B/F)}$ and F1.*Apoe*$^{-/-}$ Chr10SubJ$^{(F/F)}$ was performed using fluorescence-activated cell sorting. Comparison of Raet1 expression in aortic cell suspensions (Figure 3C and Online Figure IXC) showed that there was less Raet1 protein on the surface of endothelial cells (CD45$^-$, CD31$^+$) obtained from F1.*Apoe*$^{-/-}$ Chr10SubJ$^{(F/F)}$ mice than from F1.*Apoe*$^{-/-}$ Chr10SubJ$^{(B/F)}$ mice. This reinforces the results obtained in the *Raet1e* gene expression analysis showing not only that the *Raet1e* gene expressed poorly in aortas of SubJ$^{(F/F)}$ mice but also that aortas from SubJ$^{(F/F)}$ mice show a decreased amount of surface Raet1 protein compared with SubJ$^{(B/F)}$ mice.

Effects of *Raet1e* BAC Transgene on Atherosclerosis

The results presented thus far strongly indicate that differences in the expression of *Raet1e* gene are responsible for the atherosclerosis-susceptible locus *Ath11* 10b region. To provide additional evidence, we created BAC-transgenic mice that carried the C57 allele of *Raet1e*. To avoid the *Sgk1* gene present in the entire BAC clone RP23-149B5 (235 802 bp; Online Figure X), we microinjected a fragment of the C57-BAC clone (56 016 bp) into FVB oocytes (Figure 4A). Of the 3 different Tg*Raet1e* mouse lines that were obtained, only 1, clone Raet1e22 (TgR22), showed transgene expression in aorta and liver, whereas the other 2, clones TgR26 and TgR30, showed transgene expression in liver but not in aorta (Online Figure XI).

Because of its aortic expression, we initially used the TgR22 mouse line to determine the effect of the *Raet1e* transgene on atherosclerosis. Aortic root lesion area was assessed in F1 SubJ$^{(B/F)}$ mice with or without the *Raet1e* transgene (F1.*Apoe*$^{-/-}$ Chr10SubJ$^{(B/F)}$ Tg*Raet1e* and F1.*Apoe*$^{-/-}$ Chr10SubJ$^{(B/F)}$) and in F1 SubJ$^{(F/F)}$ mice with or without the *Raet1e* transgene (F1.*Apoe*$^{-/-}$ Chr10SubJ$^{(F/F)}$ Tg*Raet1e* and F1.*Apoe*$^{-/-}$ Chr10SubJ$^{(F/F)}$; detailed information about the cross to obtain these 4 groups of mice is described in Methods and in Online Figure Xb). In both sexes, in the absence of the BAC *Raet1e* transgene, F1.*Apoe*$^{-/-}$ Chr10SubJ$^{(F/F)}$ mice had significantly larger lesions than F1.*Apoe*$^{-/-}$ Chr10SubJ$^{(B/F)}$ mice. However, in both sexes, the presence of the BAC *Raet1e* transgene in SubJ$^{(F/F)}$ mice (F1.*Apoe*$^{-/-}$ Chr10SubJ$^{(F/F)}$ TgR22) significantly decreased the size of the lesions. No effect of the BAC *Raet1e* transgene on lesion size was observed in SubJ$^{(B/F)}$ mice (Figure 4B and 4C), presumably because *Raet1e* expression was already high in these mice.

In similar experiments, we examined the effect of the *Raet1e* transgene on atherosclerosis using mouse lines TgR26 and TgR30, which did not express C57-*Raet1e* in aorta. As shown in Online Figure XII, no effect on atherosclerotic lesion size was observed in these mouse lines. For all *Raet1e* transgenic lines, the presence of the *Raet1e* transgene did not change total and HDL cholesterol levels (Online Table IV).

These experiments confirm the identification of the *Raet1e* gene as the atherosclerosis modifier gene in the *Ath11* 10b region locus and strongly suggest that the effect of *Raet1e* on atherosclerosis requires aortic expression.

Raet1e Promoter Analysis

Because the results reported in this article strongly relate differences in *Raet1e* gene expression to differences in atherosclerosis susceptibility, we investigated the functionality of the *Raet1e* promoter to identify the molecular basis of the difference in the expression discovered between F1.*Apoe*$^{-/-}$ Chr10SubJ$^{(B/F)}$ and F1.*Apoe*$^{-/-}$ Chr10SubJ$^{(F/F)}$ mice.

Detailed analysis of mouse mRNA and expression sequence tag databases revealed that the *Raet1e* gene has multiple potential TSS (Figure 5A). To identify the predominant aortic

promoter of *Raet1e* gene, the *Raet1e*-specific rapid amplification of 5′ end of cDNA polymerase chain reaction rapid amplification of cDNA (5′RACE-PCR) assay was developed, and the results are shown in Figure 5B and 5C. The 2 most abundant aortic *Raet1e* transcripts shared the initial exon, the 5′-UTR exon 1A, and the same TSS, TSS1, but differed in the incorporation of the 5′-UTR exon 3. Taking TSS1 as the predominant *Raet1e* TSS in aorta delimits the aortic *Raet1e* promoter to a TATA-less promoter in a genomic region spanning 4.1 kb between the pseudogene Gm4895 and the TSS1. Sequence comparison of this region between C57 and FVB strains revealed 28 sequence variations.

To identify the sequence variations responsible for the differential expression in the *Raet1e* gene, different *Raet1e* promoter fragments with C57 and FVB sequences were cloned into a luciferase reporter gene vector. These constructs were transfected into C57sv002 cells (cells with C57 genetic background), and luciferase activity was compared (Online Figure XIII). As observed in vivo, promoters consisting of FVB sequence showed reduced activity compared with those with C57 sequence. This analysis also identified the promoter D fragment (1067 bp) as the minimal genomic fragment with promoter activity (Online Figure XIII), which narrowed the number of sequence variations potentially responsible for the differences in promoter activity observed between the C57 and FVB promoters to 10.

This region was further narrowed using chimeric promoter D regions, which contained a distal 781-bp C57 sequence and a proximal region 426-bp FVB sequence and vice versa. This experiment identified the first 426 bp of the *Raet1e* promoter as the region that contains the sequence variations causative of the differences in *Raet1e* expression (Figure 6A).

To analyze the functionality of the 4 sequence variations contained in this region, we used site-directed mutagenesis to modify the sequence in these positions and assessed the luciferase activity of each sequence variation. As shown in Figure 6A, the SNP rs50817078 was the only sequence variation that affected the promoter activity, showing a dramatic decrease in promoter functionality when a C57 promoter contained the FVB sequence in this position and an opposite large increase in promoter activity when an FVB promoter contained the C57 sequence in this position. The same effect was observed on transfecting these constructions into cells with BALB/c (BalbcSV006) or National Institutes of Health/Swiss (NIH3T3) genetic background (data not shown).

The SNP rs50817078 (JMRv10073), which involves a change of thymine in C57 to a cytosine in the FVB sequence, was localized inside the core of the transcription initiation sequence in the dominant TSS1 of the broad aortic promoter of *Raet1e* by aortic *Raet1e* 5′RACE PCR and sequence analysis (Figure 6B and 6C).

Therefore, this study identified the sequence variation (C/T) in the SNP rs50817078, located in the transcription initiation region of the *Raet1e* aortic promoter, as the molecular basis responsible for the atherosclerosis susceptibility in the *Ath11* 10b region locus by affecting the aortic *Raet1e* gene expression.

Discussion

In this study, the characterization of a new subcongenic line narrowed the interval of the *Ath11* 10b region. We also demonstrated that this atherosclerosis locus is independent of the atherosclerosis-sensitizing background, operative in both sexes, and independent of total and HDL cholesterol levels. Sequencing and gene expression analysis of the 5 genes present in this region identified *Raet1e* as the culprit gene, and our evidence suggests that lack of aortic expression of the *Raet1e* gene results in increased atherosclerosis. This was supported by studies in BAC-transgenic mice, in which aortic overexpression of *Raet1e* reversed the

atherosclerosis phenotype displayed by mice with diminished *Raet1e* expression. Furthermore, Raet1 proteins were localized in atherosclerotic lesions both in the core and on the surface of endothelial cells. Finally, functional promoter analysis identified the SNP rs50817078 in the transcription initiation region of the *Raet1e* gene as the molecular basis for the differences in aortic expression.

Raet1e belongs to the *Raet1* gene family, which encodes surface proteins that are members of the major histocompatibility complex class I–related family, including the *H60* gene family and *Mult1* in mice and *MICA, MICB*, and *ULBP* gene family in humans.[18] Raet1 proteins are thought to be either not expressed or expressed at low levels in normal cells, with their expression markedly upregulated by stress (ie, DNA damage, oxidative stress, heat shock).[19]

Raet1 proteins are ligands of the natural killer group 2, member D (NKG2D) receptor, and Raet1e is the isoform with the highest affinity for this receptor.[20] NKG2D is an activating receptor expressed on natural killer (NK) cells, subsets of T cells (NKT cells, CD8^{+} T cells, γδ T cells, and small subsets of CD4^{+} T cells), and some macrophages.[21] Raet1 activation of the NKG2D receptor in NK cells stimulates perforin production and in NKT cells stimulates the production of cytokines (interferon-γ, interleukin-12, tumor necrosis factor-α), which activate adjacent NK cells, B cells, T cells and macrophages. Both mechanisms are cytotoxic and capable of killing distressed Raet1-expressing cells.[22]

Our experiments show that aortic overexpression of *Raet1e* is atheroprotective. However, studies of Ly49a transgenic mice that are selectively deficient in NK cell activity, mice treated with αGalCer to activate NKT cells, and mice deficient in the NKT cell maturation and activating receptor CD1d suggest that NK and NKT cells are proatherogenic.[23] Therefore, our results seem paradoxical, and several explanations are possible.

In placenta[24] and tumor cells,[25] the overexpression of NKG2D ligands has been shown to cause NKG2D pathway desensitization. This has been invoked as a mechanism allowing the fetus and tumor to escape detection by the immune system. Desensitization can occur by constitutive NKG2D ligand expression causing internalization of the NKG2D receptor, making it inaccessible to ligands, or tumor shedding of soluble NKG2D ligands that serve as decoys sparing cells with NKG2D ligands on their surface.[22] Another possibility is that Raet1 interaction with atheroprotective cells, such as anti-inflammatory T-Reg cells (CD4^{+} T cells)[26] and M2 macrophages, [27] outweighs its interactions with proatherogenic NK and NKT cells and M1 macrophages. Another interesting possibility emerges from the fact that NKG2D ligand binding to the NKG2D receptor alone in the absence of costimulatory signals is insufficient for NK cell degranulation, suggesting that efficient NK cytotoxicity requires costimulatory signals.[28] One of these is the binding of the leukocyte integrin lymphocyte function–associated antigen 1 (LFA-1) to its primary ligand intercellular adhesion molecule (ICAM-1). For example, it has been shown that NK cells from LFA1–deficient mice are unable to kill target cells because of impaired conjugate formation.[29] If elevated expression of Raet1e on the surface of endothelial cells interferes with ICAM-1, then this could affect 2 important processes in atherosclerosis: blocking the cytotoxic effect of NK and NKT cells and impeding the recruitment of leukocytes into the vessel wall. Finally, it is possible that Raet1e acts in an NKG2D-independent manner activating atheroprotective pathways. It has been reported that NKG2D ligands can suppress T-cell proliferation and regulate neurogenesis by supporting progenitor cell proliferation in an NKG2D receptor–independent manner.[30,31] It is also of interest that the classical function of Raet1 to be expressed in distressed cells as a signal for elimination by the immune system is challenged by our observations and those of others[32] regarding Raet1 expression in proliferating cells and healthy tissues, implying Raet1 might serve nonimmune functions as

well or produce a more complex response modulated by microenvironmental and tissue-specific cellular signals that will synergize or antagonize NKG2D function.

The results presented here identify *Raet1e* as an atherosclerosis susceptibility gene and culminate our efforts using the forward genetic strategy of QTL mapping in mice to discover new genes and pathways in atherosclerosis. The human genes homologous to *Raet1* are located in 2 regions of human chromosome 6 (MICA and MICB in locus 6p21.33 and the ULBP family in locus 6q25.1), and the question arises regarding whether variations in these genes are associated with atherosclerotic cardiovascular risk factors, coronary artery disease, and myocardial infarction. Genome-wide association studies have revealed that multiple SNPs at both 6p21.33[33–36] and 6q25.1[37–39] are associated with these risk factors and medical conditions. Of course, one must be cautious about assigning causation to variations in the human *Raet1* homologs because of other genes in the region. This is especially true for MICA and MICB because they are located within the major histocompatibility complex-1 locus, which contains many genes and is characterized by broad linkage disequilibrium.

In summary, by extensive sequence, expression, and functional analysis, we have characterized the *Ath11* 10b locus and identified *Raet1e* as a novel atherosclerosis susceptibility gene. We showed that the SNP rs50817078 between the parental strains C57 and FVB that resides in the core of the transcription initiation region of *Raet1e* gene is the likely culprit. Further studies of *Raet1e* will be required to discern its mechanism of action in the aorta and to understand its role in atherosclerosis.

Supplementary Material

Refer to Web version on PubMed Central for supplementary material.

Acknowledgments

Nonstandard Abbreviations and Acronyms

HDL	high-density lipoprotein
NKG2D	natural killer group 2, member D
NKT	natural killer T cells
SNP	single nucleotide polymorphism
SubI	subcongenic I
SubJ	subcongenic J
TSS	transcription start site
UTR	untranslated region

References

1. Go AS, Mozaffarian D, Roger VL, et al. Heart disease and stroke statistics— 2013 update: a report from the American Heart Association. Circulation. 2013; 127:e6–e245. [PubMed: 23239837]

2. Libby P, Ridker PM, Hansson GK. Progress and challenges in translating the biology of atherosclerosis. Nature. 2011; 473:317–325. [PubMed: 21593864]

3. Lusis AJ. Genetics of atherosclerosis. Trends Genet. 2012; 28:267–275. [PubMed: 22480919]

4. Welch CL. Beyond genome-wide association studies: the usefulness of mouse genetics in understanding the complex etiology of atherosclerosis. Arterioscler Thromb Vasc Biol. 2012; 32:207–215. [PubMed: 22258903]

5. Getz GS, Reardon CA. Animal models of atherosclerosis. Arterioscler Thromb Vasc Biol. 2012; 32:1104–1115. [PubMed: 22383700]

6. Hunter KW, Crawford NP. The future of mouse QTL mapping to diagnose disease in mice in the age of whole-genome association studies. Annu Rev Genet. 2008; 42:131–141. [PubMed: 18759635]

7. Eppig JT, Blake JA, Bult CJ, Kadin JA, Richardson JE. Mouse Genome Database Group. The Mouse Genome Database (MGD): comprehensive resource for genetics and genomics of the laboratory mouse. Nucleic Acids Res. 2012; 40:D881–D886. [PubMed: 22075990]

8. Abiola O, Angel JM, Avner P, et al. Complex Trait Consortium. The nature and identification of quantitative trait loci: a community's view. Nat Rev Genet. 2003; 4:911–916. [PubMed: 14634638]

9. Drinkwater NR, Gould MN. The long path from QTL to gene. PLoS Genet. 2012; 8:e1002975. [PubMed: 23049490]

10. Dansky HM, Charlton SA, Sikes JL, Heath SC, Simantov R, Levin LF, Shu P, Moore KJ, Breslow JL, Smith JD. Genetic background determines the extent of atherosclerosis in ApoE-deficient mice. Arterioscler Thromb Vasc Biol. 1999; 19:1960–1968. [PubMed: 10446078]

11. Dansky HM, Shu P, Donavan M, Montagno J, Nagle DL, Smutko JS, Roy N, Whiteing S, Barrios J, McBride TJ, Smith JD, Duyk G, Breslow JL, Moore KJ. A phenotype-sensitizing Apoe-deficient genetic background reveals novel atherosclerosis predisposition loci in the mouse. Genetics. 2002; 160:1599–1608. [PubMed: 11973313]

12. Smith JD, James D, Dansky HM, Wittkowski KM, Moore KJ, Breslow JL. In silico quantitative trait locus map for atherosclerosis susceptibility in apolipoprotein E-deficient mice. Arterioscler Thromb Vasc Biol. 2003; 23:117–122. [PubMed: 12524234]

13. Teupser D, Tan M, Persky AD, Breslow JL. Atherosclerosis quantitative trait loci are sex- and lineage-dependent in an intercross of C57BL/6 and FVB/N low-density lipoprotein receptor–/– mice. Proc Natl Acad Sci U S A. 2006; 103:123–128. [PubMed: 16380418]

14. Teupser D, Wolfrum S, Tan M, Persky AD, Dansky HM, Breslow JL. Novel strategy using F1-congenic mice for validation of QTLs: studies at the proximal chromosome 10 atherosclerosis susceptibility locus. Arterioscler Thromb Vasc Biol. 2009; 29:678–683. [PubMed: 19251590]

15. Wolfrum S, Rodríguez JM, Tan M, Chen KY, Teupser D, Breslow JL. The mouse atherosclerosis locus at chromosome 10 (Ath11) acts early in lesion formation with subcongenic strains delineating 2 narrowed regions. Arterioscler Thromb Vasc Biol. 2010; 30:1583–1590. [PubMed: 20466976]

16. Cox A, Ackert-Bicknell CL, Dumont BL, Ding Y, Bell JT, Brockmann GA, Wergedal JE, Bult C, Paigen B, Flint J, Tsaih SW, Churchill GA, Broman KW. A new standard genetic map for the laboratory mouse. Genetics. 2009; 182:1335–1344. [PubMed: 19535546]

17. Burkhardt R, Sündermann S, Ludwig D, Ceglarek U, Holdt LM, Thiery J, Teupser D. Cosegregation of aortic root atherosclerosis and intermediate lipid phenotypes on chromosomes 2 and 8 in an intercross of C57BL/6 and BALBc/ByJ low-density lipoprotein receptor–/– mice. Arterioscler Thromb Vasc Biol. 2011; 31:775–784. [PubMed: 21252064]

18. Raulet DH. Roles of the NKG2D immunoreceptor and its ligands. Nat Rev Immunol. 2003; 3:781–790. [PubMed: 14523385]

19. Samarakoon A, Chu H, Malarkannan S. Murine NKG2D ligands:"double, double toil and trouble". Mol Immunol. 2009; 46:1011–1019. [PubMed: 19081632]

20. Carayannopoulos LN, Naidenko OV, Kinder J, Ho EL, Fremont DH, Yokoyama W. Ligands for murine NKG2D display heterogeneous binding behavior. Eur J Immunol. 2002; 32:597–605. [PubMed: 11857333]

21. Ogasawara K, Lanier LL. NKG2D in NK and T cell-mediated immunity. J Clin Immunol. 2005; 25:534–540. [PubMed: 16380817]

22. Champsaur M, Lanier LL. Effect of NKG2D ligand expression on host immune responses. Immunol Rev. 2010; 235:267–285. [PubMed: 20536569]

23. Whitman SC, Ramsamy TA. Participatory role of natural killer and natural killer T cells in atherosclerosis: lessons learned from in vivo mouse studies. Can J Physiol Pharmacol. 2006; 84:67–75. [PubMed: 16845892]

24. Hedlund M, Stenqvist AC, Nagaeva O, Kjellberg L, Wulff M, Baranov V, Mincheva-Nilsson L. Human placenta expresses and secretes NKG2D ligands via exosomes that down-modulate the cognate receptor expression: evidence for immunosuppressive function. J Immunol. 2009; 183:340–351. [PubMed: 19542445]

25. Nausch N, Cerwenka A. NKG2D ligands in tumor immunity. Oncogene. 2008; 27:5944–5958. [PubMed: 18836475]

26. Dai Z, Turtle CJ, Booth GC, Riddell SR, Gooley TA, Stevens AM, Spies T, Groh V. Normally occurring NKG2D+CD4+ T cells are immunosuppressive and inversely correlated with disease activity in juvenile-onset lupus. J Exp Med. 2009; 206:793–805. [PubMed: 19289577]

27. Mantovani A, Garlanda C, Locati M. Macrophage diversity and polarization in atherosclerosis: a question of balance. Arterioscler Thromb Vasc Biol. 2009; 29:1419–1423. [PubMed: 19696407]

28. Bryceson YT, March ME, Ljunggren HG, Long EO. Activation, coactivation, and costimulation of resting human natural killer cells. Immunol Rev. 2006; 214:73–91. [PubMed: 17100877]

29. Matsumoto G, Nghiem MP, Nozaki N, Schmits R, Penninger JM. Cooperation between CD44 and LFA-1/CD11a adhesion receptors in lymphokine-activated killer cell cytotoxicity. J Immunol. 1998; 160:5781–5789. [PubMed: 9637488]

30. Kriegeskorte AK, Gebhardt FE, Porcellini S, Schiemann M, Stemberger C, Franz TJ, Huster KM, Carayannopoulos LN, Yokoyama WM, Colonna M, Siccardi AG, Bauer S, Busch DH. NKG2D-independent suppression of T cell proliferation by H60 and MICA. Proc Natl Acad Sci U S A. 2005; 102:11805–11810. [PubMed: 16091471]

31. Popa N, Cedile O, Pollet-Villard X, Bagnis C, Durbec P, Boucraut J. RAE-1 is expressed in the adult subventricular zone and controls cell proliferation of neurospheres. Glia. 2011; 59:35–44. [PubMed: 21046555]

32. Eagle RA, Jafferji I, Barrow AD. Beyond stressed self: evidence for NKG2D ligand expression on healthy cells. Curr Immunol Rev. 2009; 5:22–34. [PubMed: 19626129]

33. Davies RW, Wells GA, Stewart AF, et al. A genome-wide association study for coronary artery disease identifies a novel susceptibility locus in the major histocompatibility complex. Circ Cardiovasc Genet. 2012; 5:217–225. [PubMed: 22319020]

34. Ehret GB, Munroe PB, Rice KM, et al. Genetic variants in novel pathways influence blood pressure and cardiovascular disease risk. Nature. 2011; 478:103–109. [PubMed: 21909115]

35. Kristiansson K, Perola M, Tikkanen E, et al. Genome-wide screen for metabolic syndrome susceptibility Loci reveals strong lipid gene contribution but no evidence for common genetic basis for clustering of metabolic syndrome traits. Circ Cardiovasc Genet. 2012; 5:242–249. [PubMed: 22399527]

36. Teslovich TM, Musunuru K, Smith AV, et al. Biological, clinical and population relevance of 95 loci for blood lipids. Nature. 2010; 466:707–713. [PubMed: 20686565]

37. Aouizerat BE, Vittinghoff E, Musone SL, Pawlikowska L, Kwok PY, Olgin JE, Tseng ZH. GWAS for discovery and replication of genetic loci associated with sudden cardiac arrest in patients with coronary artery disease. BMC Cardiovasc Disord. 2011; 11:29. [PubMed: 21658281]

38. Samani NJ, Erdmann J, Hall AS, et al. WTCCC and the Cardiogenics Consortium. Genomewide association analysis of coronary artery disease. N Engl J Med. 2007; 357:443–453. [PubMed: 17634449]

39. Yang Q, Kathiresan S, Lin JP, Tofler GH, O'Donnell CJ. Genome-wide association and linkage analyses of hemostatic factors and hematological phenotypes in the Framingham Heart Study. BMC Med Genet. 2007; 8(Suppl 1):S12. [PubMed: 17903294]

Novelty and Significance

What Is Known?

- Many genetic factors that affect atherosclerosis are unknown.

- In mouse models of atherosclerosis, quantitative trait locus (QTL) is one of the forward genetic strategies to identify new atherosclerosis-modifying genes and pathways.

- QTL *Ath11* is a complex containing 2 genetic regions, 10a and 10b.

What New Information Does This Article Contribute?

- Describes the steps necessary to successfully achieve positional cloning of a complex trait QTL in mouse.

- Identifies *Raet1e* as the atherosclerosis modifier gene underlying *Ath11* 10b.

- Identifies the molecular variation producing the altered aortic Raet1 expression responsible for the *Ath11* 10b effect on aortic root atherosclerotic lesion area.

- Identifies a new gene and pathway involving the innate immune system that modifies atherosclerosis.

Genetic factors contribute significantly to atherosclerotic disease, and many of these are unknown. Here, we describe the identification of a new gene and a new pathway involved in atherosclerosis. This gene was revealed by an unbiased forward genetic strategy, QTL mapping in a murine model of atherosclerosis. In this article, we fine-mapped the locus using subcongenic strains, screened the narrowed subcongenic region for structural and expression variation, identified the *Raet1e* gene as the culprit, and buttressed the case by transgenic complementation. We also showed the causal nucleotide variation in the promoter region of *Raet1e* gene underlying the phenotype. This work represents one of the few successes of the QTL strategy in complex diseases. Although we have not identified the mechanism of action, we discuss some plausible hypotheses by which *Raet1e* variation might affect atherosclerosis susceptibility. Our work provides a novel gene and a novel innate immune system pathway involved in atherosclerosis. Whether *Raet1e* variation contributes to common forms of atherosclerosis in human populations, the pathways affected by *Raet1e* are likely to be important for a better understanding of the condition.
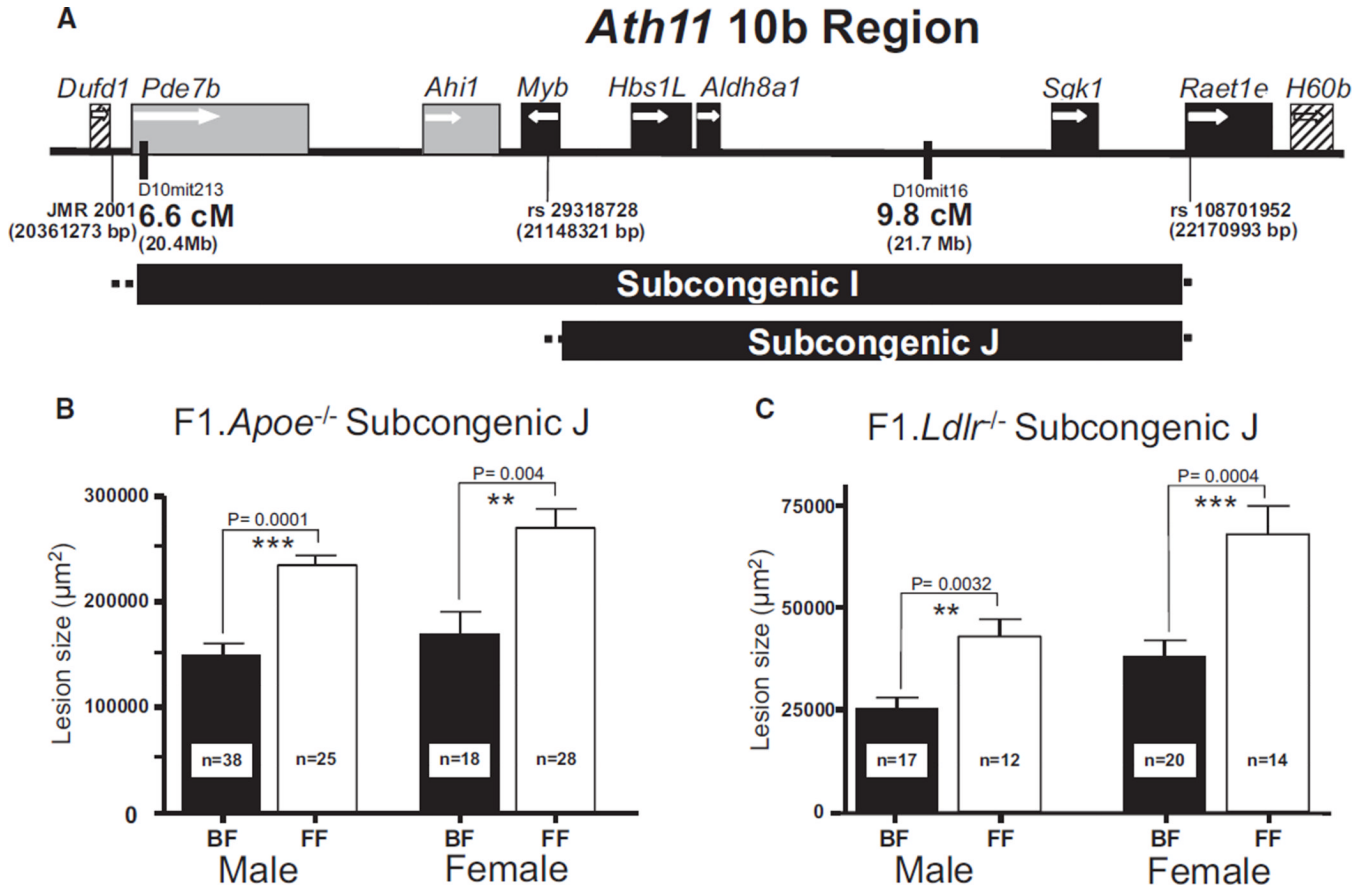
Figure 1. Subcongenic J narrows the *Ath11* 10b region

A, Schematic illustration of the subcongenic strains I and J. The horizontal bar indicates the extent of the genomic interval for each subcongenic strain. The dotted lines at either side of the bar indicate the region in which the recombination occurred. Black boxes indicate genes contained in subcongenic J. Gray boxes denote genes contained in subcongenic I but not subcongenic J. Diagonally striped boxes indicate genes outside both subcongenics. White arrows indicate the transcriptional orientation of the genes, and coordinates are based on genome assembly GRCm38. **B**, Atherosclerotic lesion area of 16-week-old F1.*Apoe*$^{-/-}$ Chr10SubJ(B/F) (BF; black column) vs F1.*Apoe*$^{-/-}$ Chr10SubJ(F/F) (FF; white column) male and female mice. **C**, Atherosclerotic lesion area of 16-week-old F1.*Ldlr*$^{-/-}$ Chr10SubJ(B/F) (BF; black column) vs F1.*Ldlr*$^{-/-}$ Chr10SubJ(F/F) (FF; white column) male and female mice. The numbers of mice studied with each genotype are indicated at the bottom of their respective columns.
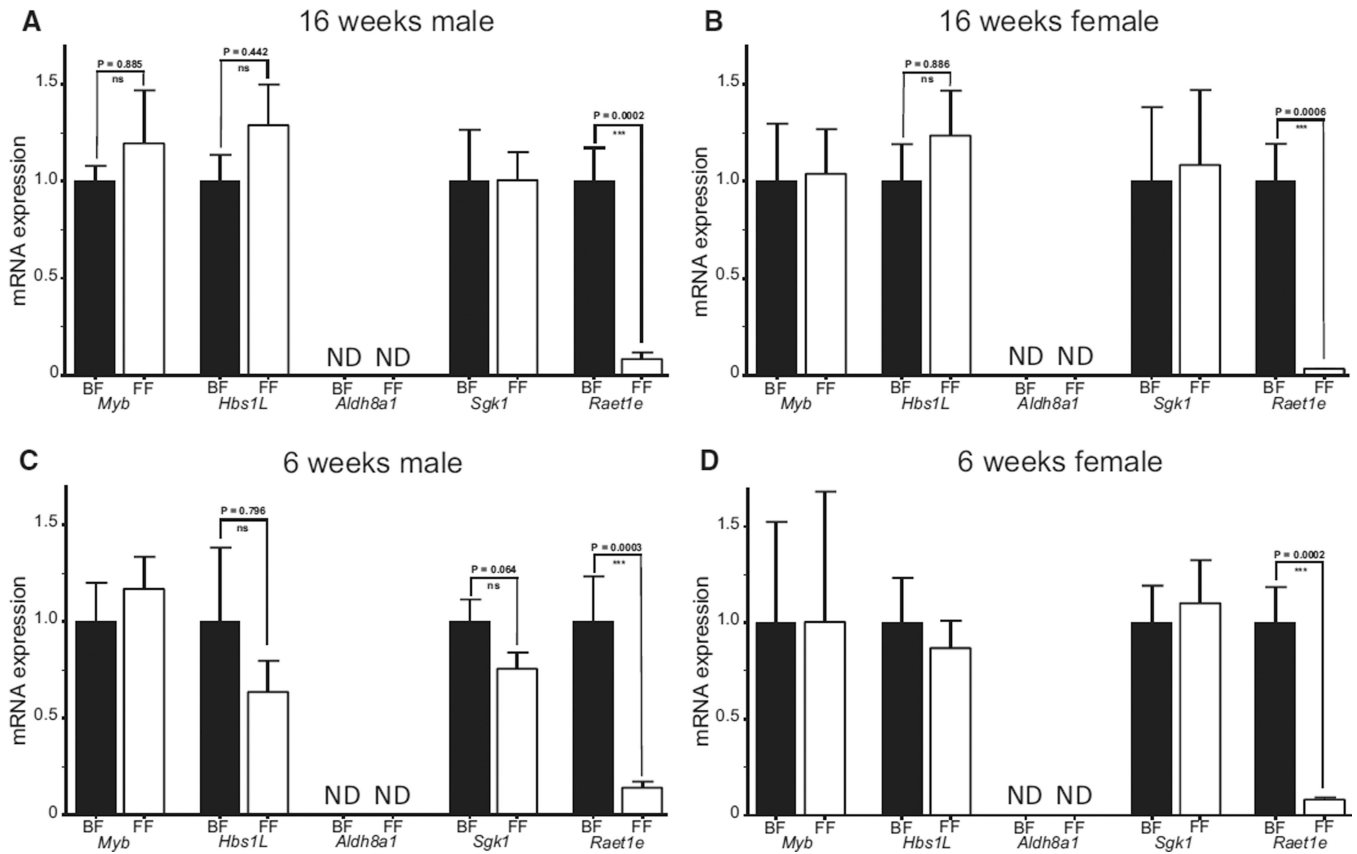
Figure 2. Aortic expression of *Ath11* 10b region genes
Aortic expression of subcongenic J genes (*Myb, Hbs1L, Aldh8a1, Sgk1*, and *Raet1e*) in 16-week-old F1.*Apoe*$^{-/-}$ Chr10SubJ(B/F) (BF; black column) vs F1.*Apoe*$^{-/-}$ Chr10SubJ(F/F) (FF; white column) male (**A**) and female (**B**) mice and in prelesional 6-week-old F1.*Apoe*$^{-/-}$ Chr10SubJ(B/F) (BF; black column) vs F1.*Apoe*$^{-/-}$ Chr10SubJ(F/F) (FF; white column) male (**C**) and female (**D**) mice. There were 14 mice per group, and the expression of each gene was normalized to the level in F1.*Apoe*$^{-/-}$ Chr10SubJ(B/F) (BF) mice. ND indicates not detected.
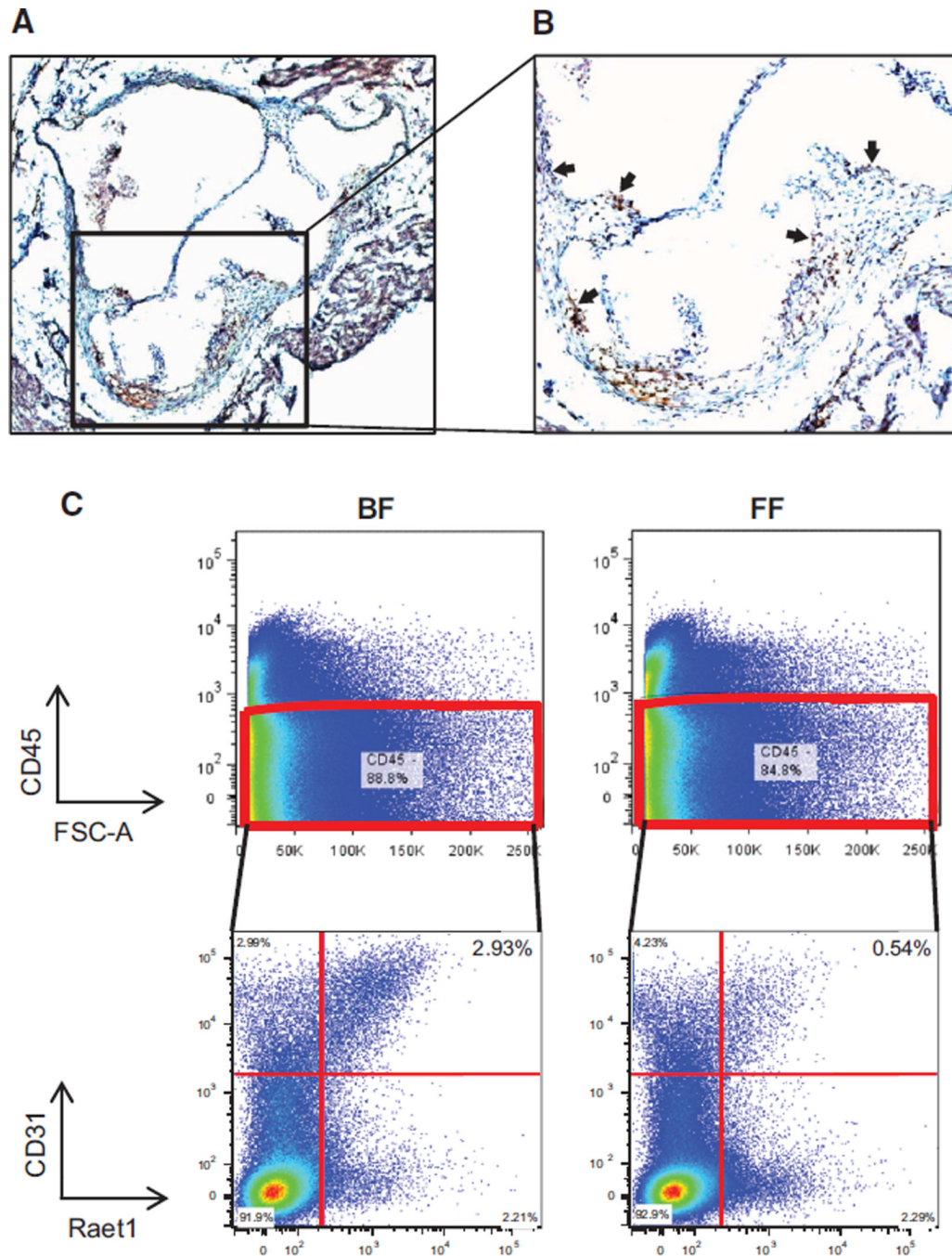
Figure 3. Raet1 protein expression in aorta

A, The ×40 and (**B**) ×100 sections of aortic root from 16-week-old F1.*Apoe*$^{-/-}$ Chr10SubJ(B/F) mice immunostained with antibody to Raet1. Brown–red areas indicate regions of Raet1 protein expression (see arrows). **C**, Fluorescence-activated cell sorting (FACS) analysis of Raet1 expression in aortic endothelial cells. Aortic cell suspensions from 16-week-old F1.*Apoe*$^{-/-}$ Chr10SubJ(B/F) (BF; **left**) and F1.*Apoe*$^{-/-}$ Chr10SubJ(F/F) (FF; **right**) mice were subjected to FACS analysis. **Top**, Separation of CD45-positive cells and CD45-negative cells. The latter were analyzed for the presence of CD31 and Raet1, and the results are shown at the **bottom**. The results shown are representative of 3 experiments.
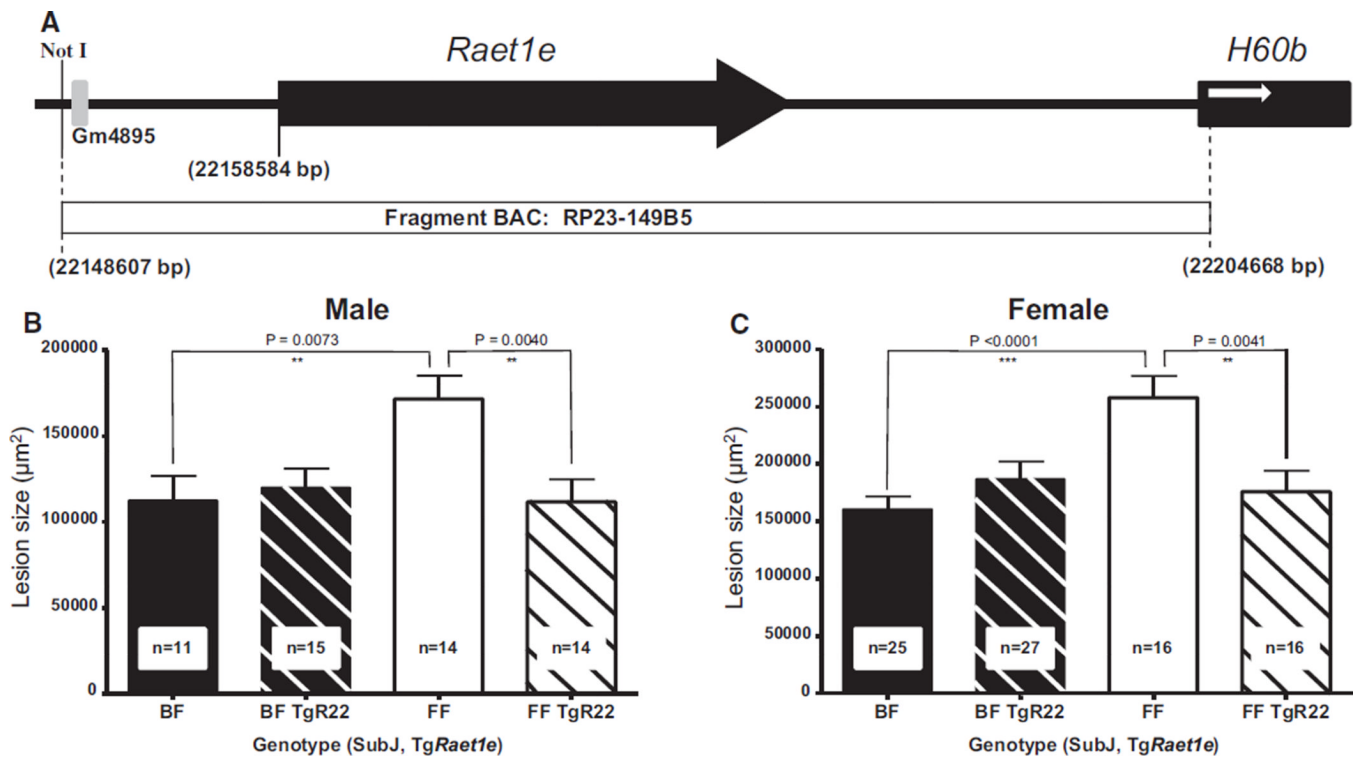
Figure 4. Creation of BAC-*Raet1e* transgenic mice and assessment of atherosclerosis
A, Not I fragment of C57 BAC RP23-149B5 containing only the *Raet1e* gene microinjected into FVB oocytes to obtain *Raet1e* transgenic mice. The black arrow indicates the extent and orientation of the *Raet1e* gene, the gray box indicates a pseudogene, the black box indicates the neighboring *H60b* gene not contained in the BAC, and the white arrow indicates its orientation. The coordinates given are based on genome assembly GRCm38. **B** and **C**, Effect of BAC-*Raet1e* transgene–driven overexpression of *Raet1e* on atherosclerosis. Atherosclerotic lesion area of F1.*Apoe*$^{-/-}$ Chr10SubJ(B/F) (BF; black column), F1.*Apoe*$^{-/-}$ Chr10SubJ(B/F) Tg*Raet1e*22 (BF TgR22; diagonally striped black column), F1.*Apoe*$^{-/-}$ Chr10SubJ(F/F) (FF; white column), and F1.*Apoe*$^{-/-}$ Chr10SubJ(F/F) Tg*Raet1e*22 (FF TgR22; diagonally striped white column) male (**B**) and female (**C**) mice. The numbers of mice studied with each genotype are indicated at the bottom of their respective columns.
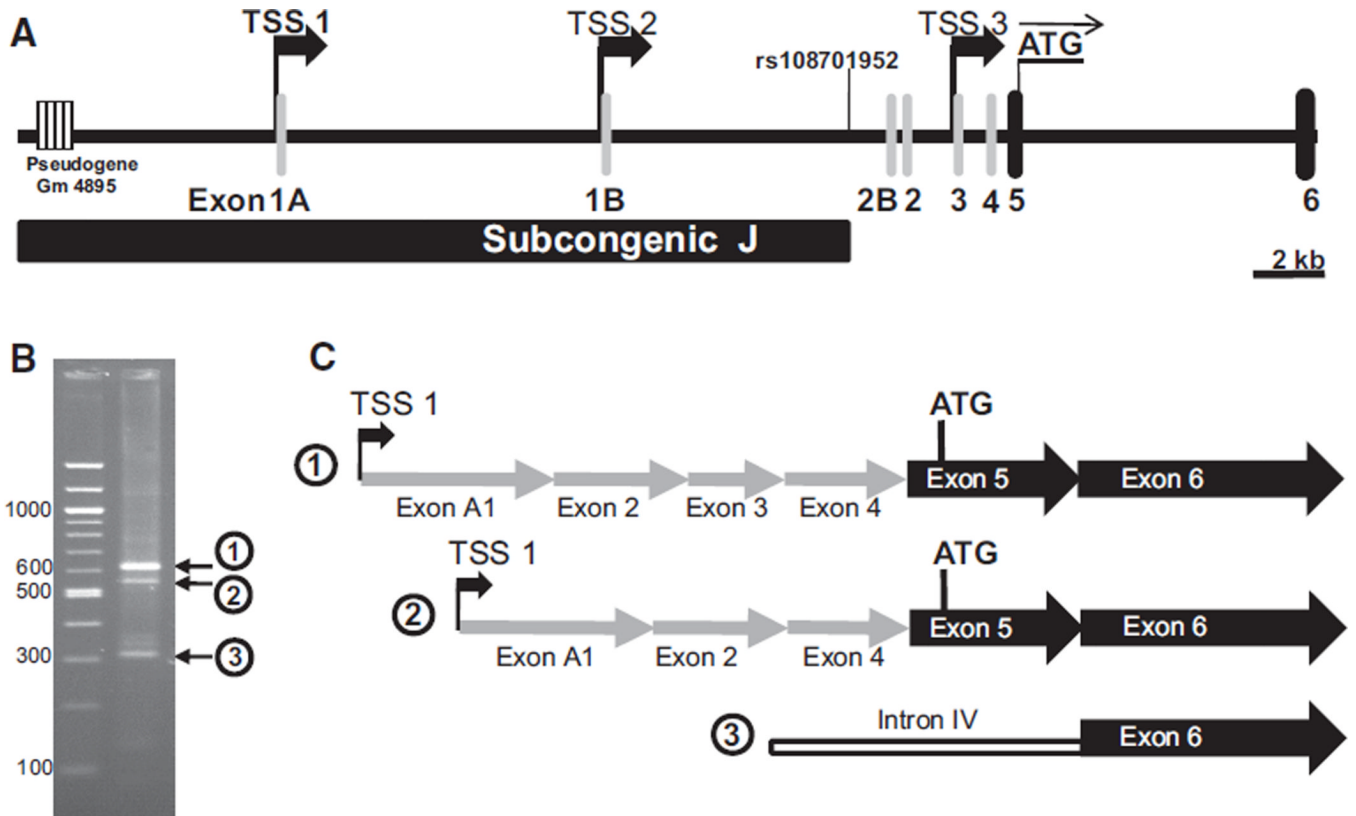
Figure 5. Identification of the *Raet1e* aortic promoter by rapid amplification of 5′ end of cDNA (5′RACE)

A, Promoter, 5′-untranslated region (UTR) and the beginning of the translated region of the *Raet1e* gene. The black bar indicates the distal end of subcongenic J delimited by the single nucleotide polymorphism rs108701952, the gray columns indicate 5′-UTR exons, the black columns indicate translated exons, the thick black arrows indicate potential transcription start sites (TSS) determined based on the expression sequence tag (EST) database, the thin black arrow indicates the translation initiation ATG codon, and the striped box indicates a pseudogene. The coordinates given are based on genome assembly GRCm38. **B**, Agarose gel electrophoresis of size markers (**left lane**) and products of the aortic *Raet1e* 5′RACE (**right lane**). The circled numbers indicate the 3 major DNA products, which were isolated and sequenced to determine the TSS. **C**, Sequence comparison of the 3 major aortic *Raet1e* 5′RACE products. The gray arrows indicate 5′-UTR exons, the black arrows indicate translated exons, and the white bar indicates an intron. Aortic *Raet1e* transcripts 1 and 2 begin at TSS1 but differ by the absence of exon 3 in the latter. Aortic *Raet1e* transcript 3 begins in the middle of the intron IV and is likely an experimental artifact.
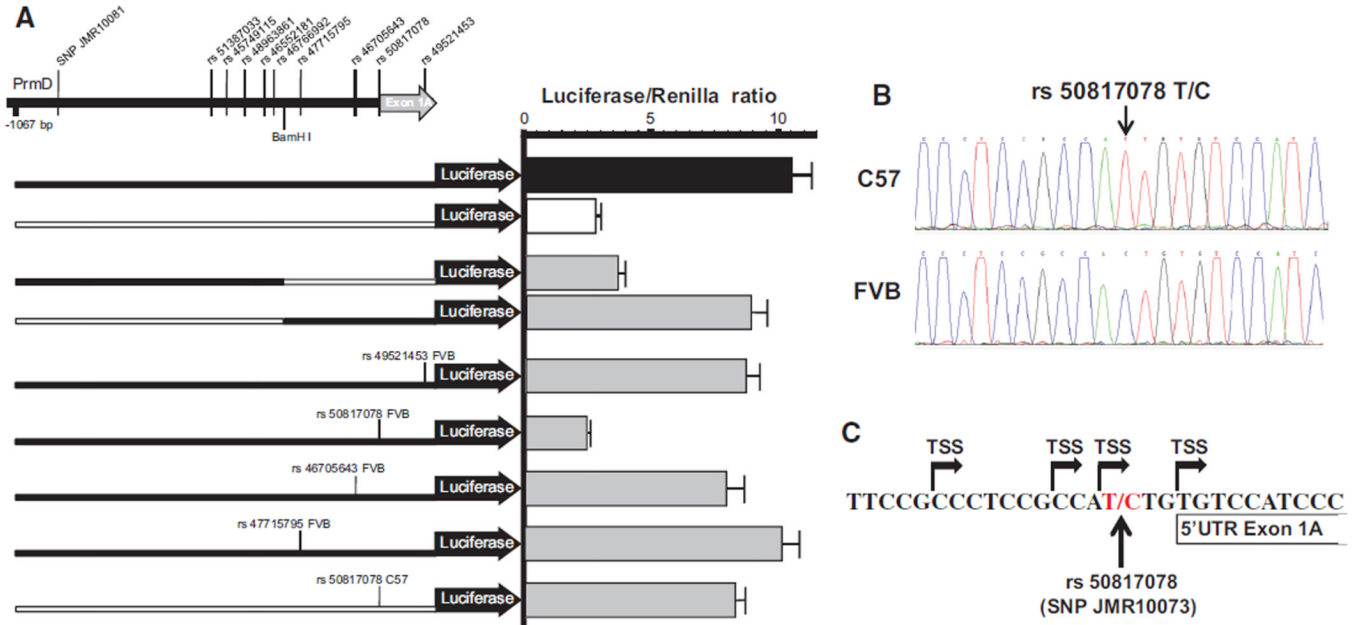
Figure 6. Analysis of functional differences in the *Raet1e* promoter between C57 and FVB
Based on the results shown in Online Figure XIII, it seems that the major difference in the
aortic expression of *Raet1e* is determined by sequence differences between C57 and FVB in
the promoter D fragment. **A, Top**, Locations of sequence differences between C57 and FVB
in the promoter D fragment. Below are the different forms of promoter D analyzed. The
black bars indicate C57 sequence, the white bars indicate FVB sequence, and the vertical
lines indicate sequence variations introduced by site-directed mutagenesis. The horizontal
bar graph indicates the ratio of luciferase/renilla activity for each promoter construct. The
black bar indicates the activity of a construct with only C57 sequence, the white bar
indicates the activity of a construct with only FVB sequence, and the gray bars designate the
activity of modified forms of the *Raet1e* promoter D. The activity ratio of luciferase/renilla
is given as mean±SEM. **B**, Chromatographic representation of the sequence difference
between C57 and FVB in the region of the culprit single nucleotide polymorphism (SNP)
rs50817078 (arrow). **C**, SNP rs50817078 (JMRv10073) localizes to the core of the aortic
Raet1e TSS1 based on the sequence obtained for transcript number 1 in Figure 5.

Table

Summary of Sequence Variations Identified in *Ath11* 10b Region Genes Comparing C57 and FVB Strains

Gene	N of Variations	SNP/Indel	Region
Myb	1	SNP (1)[*]	Promoter (1)
Hbs1L	4	SNP (3)	Promoter (3), 5′-UTR (1)
		Insertion (1)	
Aldh8a1	9	SNP (4)	Promoter (2), 3′-UTR (7)
		Insertion (4)	
		Deletion (1)	
Sgk1	6	SNP (5)	Promoter (4), exon (2 silent mutations)
		Insertion (1)	
Raet1e	138[†]	SNP (124)	Promoter (63), 5′-UTR (75)
		Insertion (6)	
		Deletion (8)	

SNP indicates single nucleotide polymorphism; and UTR, untranslated region.

[*] Number of sequence variations in parenthesis.

[†] In 19 kb sequenced, in the rest of the genes we sequenced around 4 kb.